Talanta 117 (2013) 431–437

Contents lists available at ScienceDirect

Talanta

journal homepage: www.elsevier.com/locate/talanta

A carbon nanotube screen-printed electrode for label-free detection of the human cardiac troponin T

Bárbara V.M. Silva, Igor T. Cavalcanti, Mízia M.S. Silva, Rosa F. Dutra *

Biomedical Engineering Laboratory, Federal University of Pernambuco, Av. Prof. Moraes Rego, 1235-Cidade Universitária, 50670-901 Recife, Pernambuco, Brazil

ARTICLE INFO

Article history:
Received 15 March 2013
Received in revised form
28 August 2013
Accepted 30 August 2013
Available online 6 September 2013

Keywords:
Immunosensor
Screen-printed electrode
Carbon nanotube
Human cardiac troponin T
Point-of-care testing

ABSTRACT

Label-free immunosensor based on amine-functionalized carbon nanotubes screen-printed electrode is described for detection of the cardiac troponin T, an important marker of acute myocardial infarction. The disposable sensor was fabricated by tightly squeezing an adhesive carbon ink containing carbon nanotubes onto a polyethylene terephthalate substrate forming a thin film. The use of carbon nanotubes increased the reproducibility and stability of the sensor, and the amine groups permitted nonrandom immobilization of antibodies against cardiac troponin T. Amperometric responses were obtained by differential pulse voltammetry in presence of a ferrocyanide/ferricyanide redox probe after troponin T incubation. The calibration curve indicated a linear response of troponin T between 0.0025 ng mL^{-1} and 0.5 ng mL^{-1}, with a good correlation coefficient ($r=0.995$; $p<0.0001$, $n=7$). The limit of detection (0.0035 ng mL^{-1} cardiac troponin T) was lower than any previously described by immunosensors and was comparable with conventional analytical methods. The high reproducibility and clinical range obtained using this immunosensor support its utility as a potential tool for point-of-care acute myocardial infarction diagnostic testing.

1. Introduction

Human cardiac troponin T (cTnT) is a sensitive and specific marker of cardiac injury that is regarded as the gold standard marker in the diagnosis of acute myocardial infarction (AMI). The detection of ultra-low levels of cTnT during early stages of cardiac disease facilitates the risk stratification and prognosis of the heart damage. The blood cTnT concentration rises rapidly within 3–4 h after AMI onset [1–3] and can be analyzed in the laboratory using several well-established enzymatic immunoassays based on reactions with chromogenic [4] and chemiluminescent substrates [5]. Point-of-care testing for cTnT could provide a potential analytical tool to reduce the turnaround time for assay compared with currently methods. Immunosensor technology offers a practical and simple immunoassay method for the determination of cTnT in the emergency departments.

Although immunosensors based on optic [6–9] and piezoelectric [10–12] transductions have been widely described for label-free cTnT detection, they are not suitable for point-of-care testing because they require more complex instrumentations and laborious manufacturing procedures, besides they are more expensive and difficult to miniaturize. Electrochemical transducers employing screen-printed electrodes (SPEs) have emerged as appropriate for point-of-care testing. These transducers are easily adaptable for in mass production, disposable and interchangeable with other biosensors, such as popular enzymatic glucometers [13,14]. Another advantage exhibited by the SPEs is their versatility to obtain electrodes with modifications in size and thickness by simple changing squeezing pressure, resulting in electrodes more sensitive and exhibiting improved electrochemical proprieties.

The cTnT detection in human serum by using electrochemical immunosensors has been possible by some authors [15–18]. However, the requirement of the electroactive species like the peroxidase enzyme that are dependent on Michaelis–Menten kinetic limits the immunosensor sensitivity. Moreover, the necessity for additional biochemical steps, including conjugated antibody incubations and reactions with specific substrates, increases the analysis time [19]. Recently reports have described label-free immunosensors that use voltammetric techniques, such as differential pulse voltammetry (DPV) [20,21]. This technique measures current by generating successive and regular voltage pulses superimposed on the potential linear sweep or stair steps. The current in an immunosensor is changed by antigen–antibody coupling on the electrode surface altering the mass transfer (i.e., electronic diffusion). At high potentials, DPV is limited by the high background current that hinders mass transfer and leads to a reduction in the accuracy of the amperometric response [22]. In attempting to overcome these difficulties some nanomaterials have been

* Corresponding author. Tel./fax: +55 81 2126 8000.
E-mail addresses: rosa.dutra@ufpe.br, rfiremandutra@yahoo.com.br (R.F. Dutra).

0039-9140/$ - see front matter © 2013 Elsevier B.V. All rights reserved.
http://dx.doi.org/10.1016/j.talanta.2013.08.059

proposed increasing the accuracy of immunosensors. Carbon nanotubes (CNTs) have attracted considerable attention due to their extraordinary properties, including their ability to mediate the electron-transfer reactions and to increase electrode surface area [23]. Gomes-Filho et al. [17] have proposed CNTs as alternative suggestion for the detection of serum cTnT with low limit of detection (LOD), although the conjugation of peroxidase to anti-cTnT was necessary to obtain the amperometric signal.

CNTs have been commonly deposited onto an electrode surface by simple adsorption [24] or assembled on a polymeric film [17]. However, these strategies are associated with instabilities in the response because the CNTs can leach during the measurement process. When the CNTs are incorporated into the sensor matrix (i.e., by forming nanocomposites), it is easier to control the amount of the CNTs used and to minimize their loss. Additionally, this procedure has advantage to be a one-step preparation method [25] and to dispense the use of electron-transfer mediators [26], beside CNTs act as anchors for an optimal biomolecules immobilization. Due to their facility to be functionalized with amine groups antibodies should be immobilized by Fc portion in order to expose the Fab sites to the epitopes [27]. In this study, amine functionalized CNTs were incorporated into the ink printing used to fabricate SPEs (CNT-SPE). A stable and oriented immobilization of antibodies combined with the electrochemical advantages of the CNTs allowed a rapid detection of cTnT. No labels were necessary when the antigen–antibody interactions were measured by applying DPV. The method described herein involves a straightforward preparation process and represents an advancement in the adaptation of SPEs point-of-care testing.

2. Materials and methods

2.1. Reagents and patient samples

Native cTnT purified from human cardiac muscle tissue was obtained from Calbiochem (Darmstadt, Germany). Mouse monoclonal anti-cTnT was purchased from Abcam (Cambridge, England). Amine-functionalized, multi-walled, 95% pure CNTs (NH_2-CNTs), were obtained from DropSens (Oviedo, Spain). Potassium ferricyanide ($K_3[Fe(CN)_6]$), potassium ferrocyanide ($K_4[Fe(CN)_6]$), *N*-hydroxysuccinimide (NHS), *N*-ethyl-*N*′-(3-dimethylaminopropyl) carbodiimide (EDC), dimethylformamide (DMF), and glycine were acquired from Sigma-Aldrich (St. Louis, MO, USA). Carbon ink (Electrodag PF-407C) was purchased from Acheson (Port Huron, MI, USA) for the fabrication of the CNT-SPEs. Phosphate-buffered saline (PBS) (10 mmol L^{-1}, pH 7.4) used in all experiments was prepared by dissolving 0.2 g KCl, 8.0 g NaCl, 0.24 g KH_2PO_4, and 1.44 g Na_2HPO_4 in 1000 mL of deionized Milli-Q water (from Millipore, units (Bedford, MA, USA). All chemicals were analytical grade.

Blood serum samples were collected from patients with AMI who were admitted to the Cardiac Emergency Hospital of Pernambuco—PROCAPE (Recife, Brazil). An automatic Elecsys 2010 Immunoassay Analyzer (Roche Diagnostics) was used to quantify cTnT via an electrochemical chemiluminescence immunoassay (ECLIA). Samples were stored at −20 °C while not in use during the electrochemical measurements.

2.2. Apparatus

Electrochemical measurements were performed using an Ivium CompactStat potentiostat obtained from Ivium Technologies (Eindhoven, Netherlands) that was interfaced to a computer system and controlled by Ivium software. All electrochemical measurements were made using a three-electrode system comprised of the CNT-SPE as working electrode, a helical platinum wire as auxiliary electrode, and an Ag/AgCl electrode as reference. All potentials given in this work were determined relative to the Ag/AgCl reference electrode. Electrochemical analyses were carried out using an electrochemical cell (10 mL) at room temperature (at approximately 24 °C).

Fourier transform infrared (FT-IR) spectroscopy was performed to chemically characterize the CNT-SPE. FT-IR measurements were performed in attenuated total reflectance (ATR) mode using an IFS-66 FTIR (scans=50, energy scanning from 400 cm^{-1} to 4000 cm^{-1}) acquired from Bruker (Karlsruhe, Germany).

Atomic force microscopy (AFM) was performed to characterize the morphology and topography of the CNT-SPE using an alpha300S AFM obtained from WITec (Ulm, Germany). Images were acquired in tapping mode using silicon tips at 0.2 N m^{-1} constant force.

2.3. CNT-SPE manufacturing

The CNT-SPE was fabricated by tightly squeezing an adhesive carbon ink containing NH_2-CNTs onto a polyethylene terephthalate (PET) rectangular surface to form a thin film. Prior to carbon ink incorporation, the NH_2-CNTs (5 mg) were dispersed in 1 mL of DMF and were immersed in an ultrasonic bath for 4 h until a black homogeneous suspension was obtained. A plastic mold was affixed to the rectangular PET surface (0.4 cm × 1.0 cm) to ensure SPEs with equal printed areas. After fabrication, the electrodes were cured at 60 °C for 20 min [22]. The manufactured CNT-SPE consisted of a circular area (Ø=4 mm) joined to a rectangular area (1 mm × 15 mm), which was used as an electrical contact. Prior to use, the CNT-SPE was cleaned rigorously by electrochemical pretreatment with 40 scans, in a potential between 2.0 V and −2.0 V in KCl (100 mmol L^{-1}) [28].

2.4. Anti-cTnT immobilization

Prior to immobilization, the carboxylic groups of anti-cTnT antibodies (5 μg mL^{-1}) were activated for 90 min in a solution of NHS (5 mmol L^{-1}) and EDC (2 mmol L^{-1}) prepared in PBS (10 mmol L^{-1}, pH 7.4). Afterwards, an aliquot (10 μL) of activated anti-cTnT antibodies was pipetted onto the CNT-SPE. The anti-cTnT incubation was maintained in a moist chamber at room temperature for 60 min. Finally, a glycine solution (50 mmol L^{-1}) prepared in PBS (10 mmol L^{-1}, pH 7.4) to block non-specific bindings was pipetted on the electrode for 45 min (Fig. 1a).

2.5. Electrochemical immunoassay

Antigen–antibody interactions at the interface of the CNT-SPE were monitored by DPV in real-time (Fig. 1b). DPV measurements were recorded from 0 V to 0.8 V with a pulse amplitude of 0.025 V, a width of 0.05 s, and a step potential of 0.05 V. The analytical response to cTnT was obtained taking into account the difference between the peak current (ΔI) of the CNT-SPE with cTnT and the blank (i.e. without cTnT). The current signals were registered at a fixed potential (+0.25 V).

Immunosensor preparation was characterized by cyclic voltammetry (CV) and electrochemical impedance spectroscopy (EIS) analyses. CVs were scanned from 1.0 V to −0.6 V at 50 mV s^{-1}. AC impedance measurements were performed in the frequency range from 1×10^{-2} Hz to 6.5×10^{4} Hz in a given open circuit voltage with an amplitude of 10 mV. All electrochemical measurements were conducted in $K_3[Fe(CN)_6]/K_4[Fe(CN)_6]$ (5 mmol L^{-1}) prepared in PBS (10 mmol L^{-1}, pH 7.4).

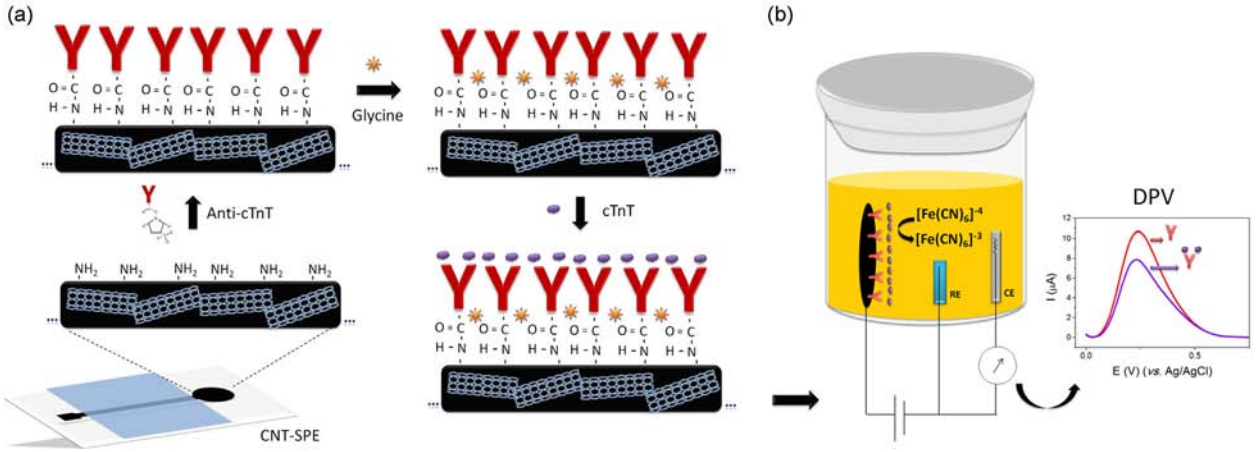

Fig. 1. Schematic representation of the (a) immunosensor fabrication and (b) electrochemical principle of detection.

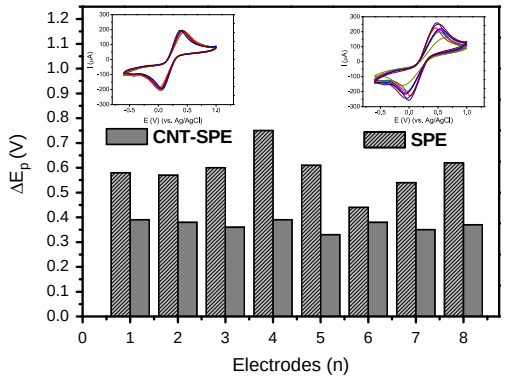

Fig. 2. ΔEp of the eight SPEs with and without NH_2-CNT. *Inset*: CVs of the electrodes with and without NH_2-CNT in presence of the $K_3[Fe(CN)_6]/K_4[Fe(CN)_6]$ (5 mmol L^{-1}) prepared in PBS (10 mmol L^{-1}, pH 7.4) at 50 mV s^{-1} scan rate.

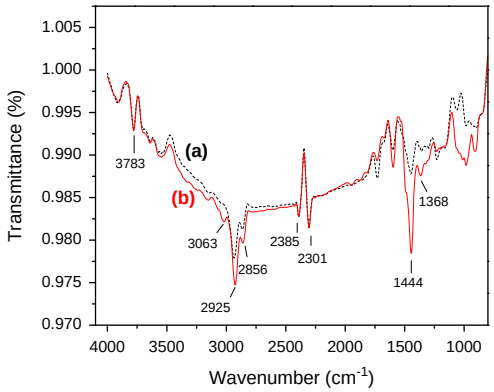

Fig. 3. ATR FT-IR spectra of the SPE (a) without NH_2-CNT and (b) with NH_2-CNT.

3. Results and discussion

3.1. Effect of NH_2-CNTs on the SPE

The electrochemical profile of the SPE with and without NH_2-CNTs incorporated into the carbon ink matrix was investigated initially using CVs. The influence of NH_2-CNTs on the redox peak-to-peak separation (ΔEp) is shown in Fig. 2. SPEs with NH_2-CNT exhibited a lower ΔEp (0.38 V) than those without NH_2-CNTs (0.58 V), suggesting greater electron transfer. A lower relative standard deviation (RSD) was observed in SPEs with NH_2-CNTs (2.1%) in comparison to without NH_2-CNTs (8.7%), indicating an increased reproducibility. Additionally, a higher reversibility of the redox peaks was obtained with NH_2-CNTs, suggesting improved homogeneity and regularity of the carbon ink film on the electrode surface [29,27].

FT-IR spectra were used to investigate the modification of the carbon ink with NH_2-CNTs (5 mg mL^{-1}). The FT-IR spectra of the carbon ink layer without NH_2-CNTs are shown in Fig. 3a. The peak at 3783 cm^{-1} corresponds to the band of hydroxyl groups. The peaks at 2925 cm^{-1} and 2856 cm^{-1} reveal asymmetric and symmetric stretches corresponding to methyl and methylene groups, respectively. These bands are attributed to the ethylene glycol ether present in the ink [30]. The peaks at 2385 cm^{-1} and 2301 cm^{-1} are attributed to C–H stretching vibrations of alkyne groups. After incorporation of the NH_2-CNTs in the carbon ink (Fig. 3b), two peaks were observed at 2925 cm^{-1} and 2856 cm^{-1} corresponding to methyl and methylene groups, respectively [31]. It was also observed the presence of peaks corresponding to amino groups at 1444 cm^{-1} and 1368 cm^{-1} that could be attributed to the presence of NH_2-CNTs in the carbon ink [21].

AFM was used to characterize the morphology of the CNT-SPEs. The topographic surface of the CNT-SPE was characterized by amorphous structures typical of polymeric films with an average roughness of 272.5 nm (Fig. 4a). After electrochemical pretreatment, the average roughness decreased to 124.4 nm (Fig. 4b) due to the removal of impurities and organic contaminants on the sensor surface. When anti-cTnT antibodies were pipetted onto the electrode surface (10 μL, 5 μg mL^{-1}) and incubated for 60 min, the average roughness increased to 273.1 nm, confirming that the anti-cTnT antibodies had been successfully immobilized (Fig. 4c).

3.2. Immobilization of the anti-cTnT

The amine groups of the CNTs were used to promote a covalent immobilization of the anti-cTnT antibodies via amide bonds. For this procedure, the Fc terminal of the anti-cTnT antibodies were activated by EDC/NHS mixing. EDC reacts with the carboxyl groups of the antibodies to form amine-reactive *o*-acylisourea intermediates. Addition of NHS stabilizes the amine-reactive intermediate and increases the efficiency of EDC-mediated coupling reactions. In situ activation of anti-cTnT antibodies yields NHS-ester-terminated Fc regions that are susceptible to nucleophilic attack from amines on the electrode surface to form stable amide bonds [32]. Oriented anti-cTnT immobilization by Fc terminal improves the sensitivity and selectivity of the immunosensor by exposing the Fabs, which exhibit a high affinity towards epitopes of the cTnT antigens.

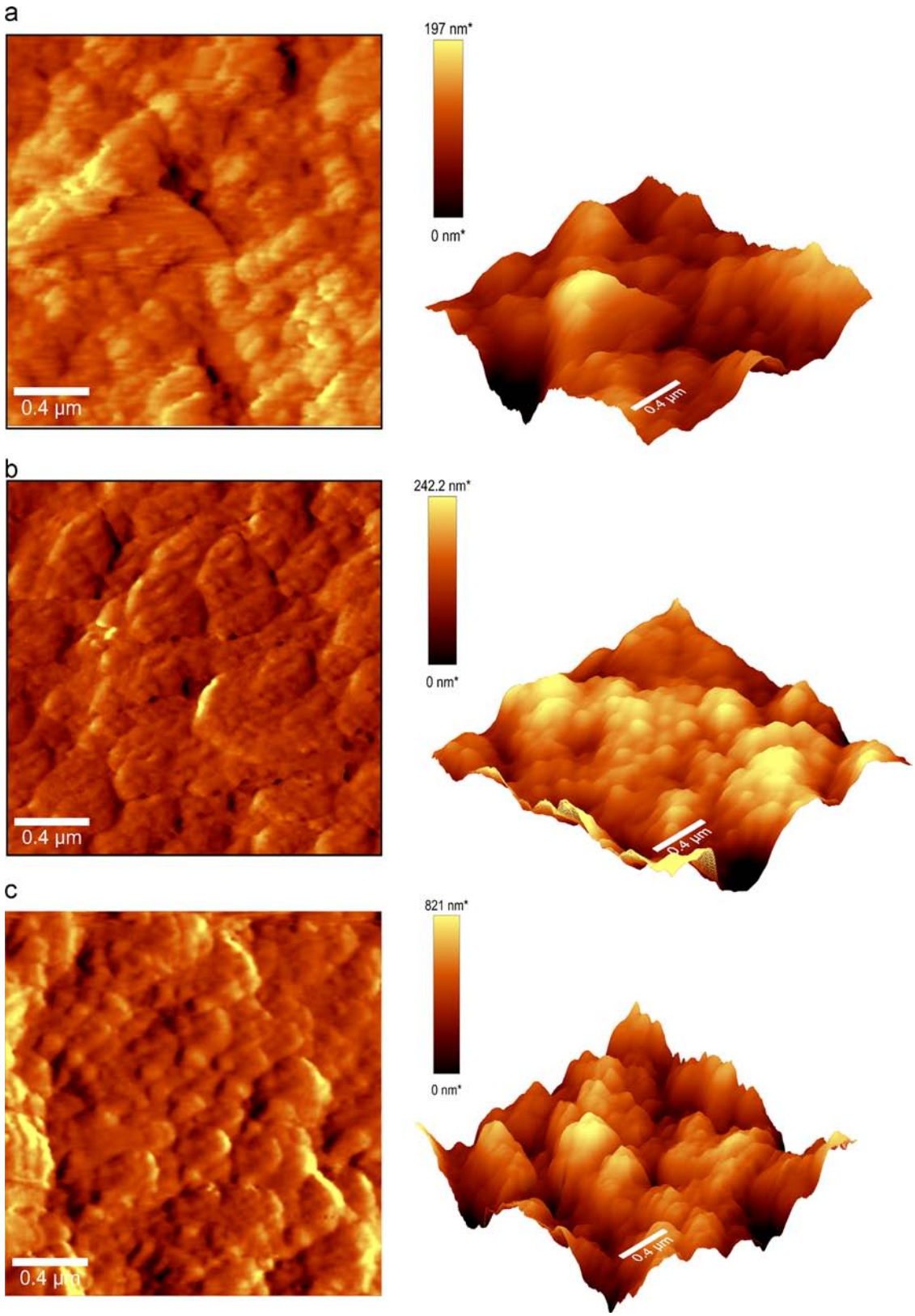

Fig. 4. 2D and 3D AFM images of the CNT-SPE (a) as manufactured, (b) after electrochemical pretreatment and (c) after anti-cTnT immobilization.

The amount of antibody immobilized on the electrode surface also affects the sensitivity of the immunosensor. In order to obtain a maximal efficiency on the attached anti-cTnT to electrode surface, the exposure time to the EDC/NHS by anti-cTnT was optimized. Herein, the exposure time ranged from 15 min to 120 min with anti-cTnT at 5 $\mu g\ mL^{-1}$. It was observed an increase of the exposure time with increase of the DPV peaks, reaching a plateau at 90 min (Fig. S1—Supplementary data). In this instant, a maximal amount of anti-cTnT Fc portions were activated resulting in more amide bonds with the NH_2-CNTs.

3.3. Assembling the SPE

In Fig. 5a, the CV of the CNT-SPE as manufactured shows a ΔE_p of 0.68 V (curve I). After electrochemical pretreatment (curve II), the ΔE_p decreased to 0.38 V, which illustrates a decrease of electron transfer resistance by removing of organic contaminants or impurities from the electrode surface. On the other hand, when the anti-cTnT was pipetted on the CNT-SPE it was, observed a decrease in the redox peaks as a result of electron-transfer inhibition due to the insulating nature of the antibody (curve III). The blocking effect to non-specific binding was observed after incubation with glycine (50 mmol L^{-1}) (curve IV). The negatively charged glycine acts by hindering the electron transfer between the anionic species of the electrolyte and the electrode surface, as demonstrated by a slight reduction in redox peaks.

CNT-SPE assembly also was evaluated by EIS. The electrodes were submitted to an electrochemical cell with $K_3[Fe(CN)_6]/K_4[Fe(CN)_6]$ (5 mmol L^{-1}) prepared in PBS (10 mmol L^{-1}, pH 7.4). According to the Nyquist plot showed in Fig. 5b, it was observed, after electrochemical pretreatment a reduction in the charge-transfer resistance (R_{ct}) from 5805 Ω (curve I) to 665 Ω (curve II), by decreasing the diameter of the semicircles. Immobilization of the anti-cTnTs were confirmed by an increase in the R_{ct} (768 Ω, curve III), due to their insulating nature. Glycine, the blocking agent, also was linked on the electrode surface as confirmed by an increase in the diameter of the semicircle (R_{ct}=966 Ω, curve IV). These results are in accordance with those obtained using CV.

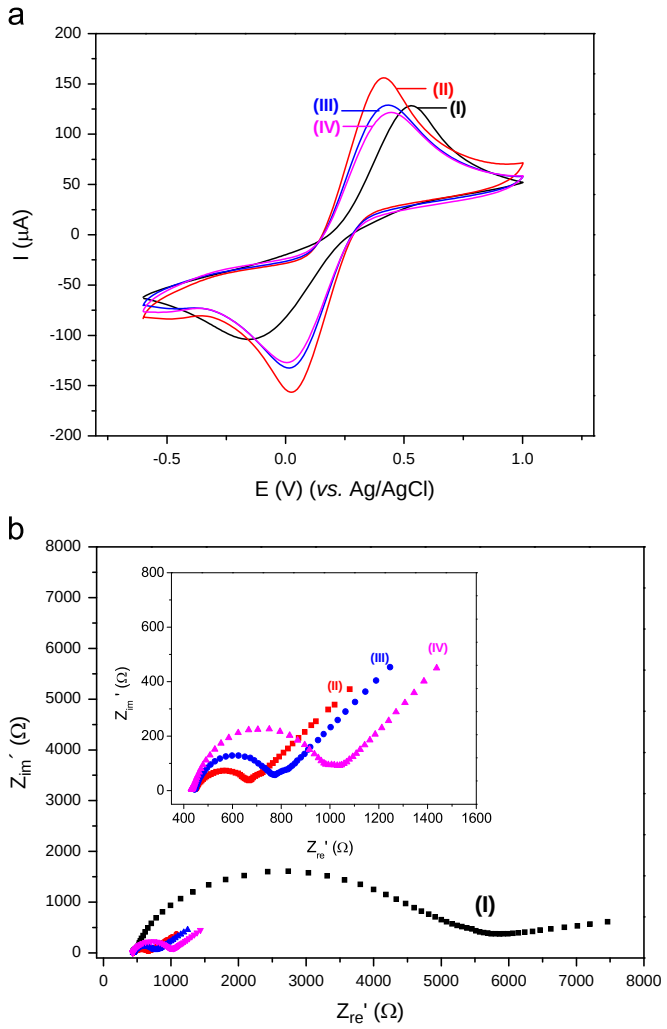

Fig. 5. Stepwise the CNT-SPE preparation: (curve I) as manufactured, (curve II) after electrochemical pretreatment, (curve III) anti-cTnT/CNT-SPE, (curve IV) glycine/anti-cTnT/CNT-SPE (a) CVs and (b) Nyquist plots in $K_3[Fe(CN)_6]/K_4[Fe(CN)_6]$ (5 mmol L^{-1}) prepared in PBS (10 mmol L^{-1}, pH 7.4).

In order to study electron diffusion at the sensor interface, glycine/anti-cTnT/CNT-SPEs were submitted to different scan rates. The electrodes were immersed in an electrochemical cell containing $K_3[Fe(CN)_6]/K_4[Fe(CN)_6]$ (5 mmol L^{-1}) in PBS (10 mmol L^{-1}, pH 7.4) as the redox probe, and voltammograms were registered (Fig. S2—Supplementary data). The currents of the anodic peak (I_{pa}) and the cathodic peak (I_{pc}) increased linearly with the square root of the scan rate (Fig. S2—Supplementary data, inset). The following linear regression equations then were calculated: $I_{pa}=14.857\nu^{1/2}+21.502$ ($r=0.999$) and $I_{pc}=-14.035\nu^{1/2}-33.578$ ($r=0.996$). These equations suggested a diffusion-controlled process. The electroactive surface area of the glycine/anti-cTnT/CNT-SPE was calculated according to the Randles–Sevcik equation [22] to be 0.047 cm^2.

3.4. Experimental conditions

Optimal experimental conditions for immunosensor detection were investigated according to the pH and ionic strength of the buffer (PBS). Electrostatic intermolecular forces of the electrolyte can affect electron transfer on the electrode surface [33]. The pH of PBS (10 mmol L^{-1}) was varied from 5.5 to 8.0; the current increased proportionately with the pH achieving a maximal current peak at pH 6.5 (Fig. S3a—Supplementary data). Therefore, pH 6.5 was adopted for all remaining measurements. The ionic strength was varied from 0.01 mmol L^{-1} to 10 mmol L^{-1}, and steady state was achieved at 5 mmol L^{-1} (Fig. S3b—Supplementary data).

Additional parameters affecting immunosensor performance include the immobilized antibody load and the incubation time of the cTnT. The anti-cTnT antibody concentration was varied from 0.01 μg mL^{-1} to 10 μg mL^{-1}. The current response to a fixed concentration of cTnT (0.05 ng mL^{-1}) in PBS was proportional to the anti-cTnT concentration with a plateau at approximately 5 μg mL^{-1} anti-cTnT (Fig. S4a—Supplementary data). At this anti-cTnT concentration, a 40 min incubation time was optimal as demonstrated by a plateau in the curve (Fig. S4b—Supplementary data), which suggested maximal antigen–antibody interaction.

3.5. Analytical response to the cTnT

Under optimized experimental conditions, the calibration curve of the immunosensor was obtained. The electrodes were incubated in various concentrations of cTnT for 40 min and then were submitted to DPV measurements in the presence of $K_3[Fe(CN)_6]/K_4[Fe(CN)_6]$ (5 mmol L^{-1}) in PBS (5 mmol L^{-1}, pH 6.5). The calibration curve indicated a gradual decrease in DPV current peaks with increased cTnT concentrations (Fig. 6a). When the data were adjusted to a linear regression equation, $\Delta I=3.25*C_{cTnT}+4.2$, a correlation coefficient of 0.995 ($p<0.0001$, $n=7$) and a low relative error ($\ll 1\%$) were obtained (Fig. 6a, inset). Based on the RSD of the blank and the slope of the calibration curve, the LOD was calculated as: LOD=3(RSD/slope) [34]. CNT-SPEs exhibited a lower LOD (0.0035 ng mL^{-1}) than previously described for cTnT electrochemical immunosensors [15–18]. One of limitations encountered for these labeled immunosensors is associated with the interaction or passivation of the electrode by requirement of an enzyme substrate or chemical mediator [35]. Moreover, limitations related to Michaelis–Menten kinetic imply an increase in the analyses time and a reduced sensitivity.

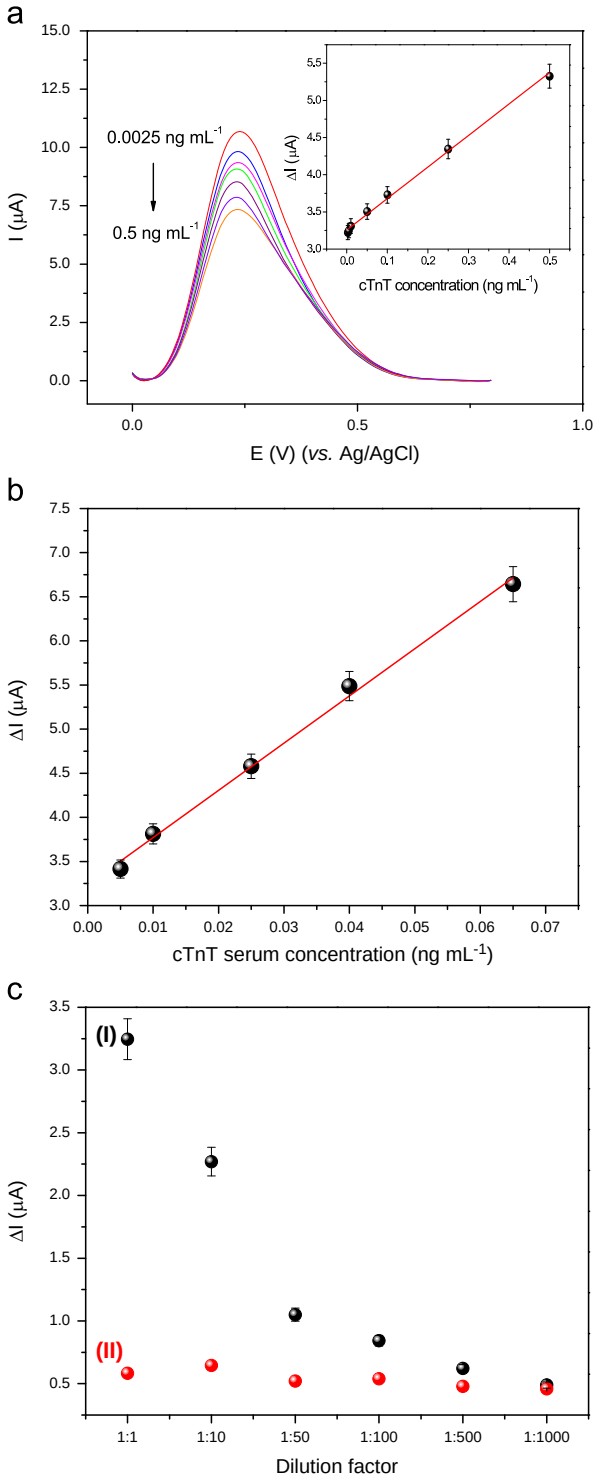

Fig. 6. (a) DPVs of immunosensor response to different the cTnT concentrations (0.0025 to 0.5 ng mL^{-1}) in presence of $K_3[Fe(CN)_6]/K_4[Fe(CN)_6]$ (5 mmol L^{-1}) in PBS (5 mmol L^{-1}, pH 6.5). *Inset*: linear fit of the calibration curve. (b) Analytical CNT-SPE responses to the cTnT measured in serum samples and (c) matrix effect study performed by successive serum dilution of samples from (curve I) myocardial infarcted and (curve II) non-myocardial infarcted patients. Error bars are based on the standard deviation of three replicates.

3.6. Repeatability and reproducibility

The repeatability of the CNT-SPE was evaluated by replicate measurements of a single electrode in response to 0.05 ng mL^{-1} cTnT under optimized experimental conditions. An RSD value of 3.2% was found for five successive determinations corresponding to a good repeatability of the immunosensor. The reproducibility was also evaluated using ten CNT-SPEs manufactured on different days and measured in response to 0.05 ng mL^{-1} cTnT. The obtained RSD was 3.8%, which implies a good reproducibility and repeatability in the fabrication procedures.

3.7. Determination of cTnT in serum samples

Fig. 6b shows the amperometric responses of the CNT-SPEs to cTnT serum samples. The immunosensor measurements were compared with those using ECLIA. The results showed good agreement with ECLIA at a 95% confidence level when the paired *t*-test was applied. The calibration plot exhibited a good linear correlation ($r=0.990$, $p<0.0001$), and a linear range of detection was observed between 0.005 ng mL^{-1} and 0.065 ng mL^{-1} cTnT. This range is comparable to the clinical range, which is associated with a cutoff of 0.01 ng mL^{-1} cTnT [36]. The LOD of CNT-SPEs for cTnT in serum samples was found to be approximately 0.007 ng mL^{-1}.

The matrix effect on the analytical response of CNT-SPEs also was evaluated (Fig. 6c). Blood serum from a non-myocardial infarction subject was diluted 1:1, 1:10, 1:50, 1:100, 1:500, and 1:1000 and then was compared to a myocardial infarction subject's serum, containing 0.01 ng mL^{-1} cTnT. All dilutions were carried out using PBS (10 mmol L^{-1}, pH 7.4). The serum dilution curve obtained from the non-myocardial infarction subject (curve I) was maintained practically constant, showing a non-matrix effect. This proposed label-free immunosensor is simpler, more rapid, and more practical for cTnT detection in blood serum and can be carried out by one-step manufacturing in addition to low cost requirements.

4. Conclusions

A disposable CNT-SPE was developed for the measurement of cTnT in blood serum. The incorporation of NH_2-CNT into the carbon ink enabled a more stable measurement and an oriented anti-cTnT immobilization leading to a high sensitivity. Additionally, the platform dispensed chemical mediators, compounds or polymers to anchor the CNTs. The CNT-SPE described in this study achieved a high sensitivity and a low LOD (0.0035 ng mL^{-1}) of cTnT compared to others electrochemical immunosensors. The linear range was obtained within cTnT clinical levels for AMI diagnostics, although further validation studies with real samples are required before clinical use.

Acknowledgements

This work was supported by the National Council for Scientific and Technological Development (CNPq) agency from Brazil. Bárbara V.M. Silva thanks to Coordination for Enhancement of Higher Education Personnel (CAPES), Brazil foundation, for the scholarship during this work. The assistance of the Northeast Center for Strategic Technologies (Recife, Brazil) and Central Analytical of Federal University of Pernambuco (Recife, Brazil) are also acknowledged.

Appendix A. Supplementary material

Supplementary data associated with this article can be found in the online version at http://dx.doi.org/10.1016/j.talanta.2013.08.059.

References

[1] J.S. Alpert, K. Thygesen, E. Antman, J.P. Bassand, J. Am. Coll. Cardiol. 36 (2000) 959–969.
[2] K. Thygesen, J.S. Alpert, H.D. White, Eur. Heart J. 28 (2007) 2525–2538.
[3] S. Mendis, K. Thygesen, K. Kuulasmaa, S. Giampaoli, M. Mahonen, K Ngu Blackett, L. Lisheng, Int. J. Epidemiol. 40 (2011) 139–146.
[4] H.A. Katus, A. Remppis, S. Looser, K. Hallermeier, T. Scheffold, W. Kubler, Mol. Cell. Cardiol. 21 (1989) 1349–1353.
[5] G. Klein, M. Kampmann, H. Baum, T. Rauscher, T. Vukovic, K. Hallermayer, H. Rehner, M. Müller-Bardorff, H.A. Katus, Wien. Klin. Wochenschr. 110 (1998) 40–51.
[6] R.F. Dutra, R.K. Mendes, V. Lins da Silva, L.T. Kubota, J. Pharm. Biomed. Anal. 43 (2007) 1744–1750.
[7] R.F. Dutra, L.T. Kubota, Clin. Chim. Acta 376 (2007) 114–120.
[8] H. Andersson, B. Kågedal, C.-F. Mandenius, Anal. Bioanal. Chem. 398 (2010) 1395–1402.
[9] J.T. Liu, C.J. Chen, T. Ikoma, T. Yoshioka, J.S. Cross, S.J. Chang, J.Z. Tsai, J. Tanaka, Anal. Chim. Acta 703 (2011) 80–86.
[10] K. Wong-ek, O. Chailapakul, N. Nuntawong, K. Jaruwongrungsee, A. Tuantranont, Biomed. Tech. (Berlin) 55 (2010) 279–284.
[11] R.A. Fonseca, J. Ramos-Jesus, L.T. Kubota, R.F. Dutra, A Nanostructured, Sensors 11 (2011) 10785–10797.
[12] A.B. Mattos, T.A. Freitas, V. Lins da Silva, R.F. Dutra, Sens. Actuators, B 161 (2012) 439–446.
[13] J. Wang, Chem. Rev. 108 (2008) 814–825.
[14] V. Gubala, L.F. Harris, A.J. Ricco, M.X. Tan, D.E. Williams, Anal. Chem. 84 (2012) 487–515.
[15] B.M.V. Silva, I.T. Cavalcanti, A.B. Mattos, P. Moura, M. del, P. Sotomayor, R. F. Dutra, Biosens. Bioelectron. 26 (2010) 1062–1067.
[16] B. Esteban-Fernández de Ávila, V. Escamilla-Gomez, S. Campuzano, M. Pedrero, J.M. Pingarrón, Electroanalysis 24 (2012) 1–8.
[17] S.L.R. Gomes-Filho, A.C.M.S. Dias, M.M.S. Silva, B.V.M. Silva, R.F. Dutra, Microchem. J. 109 (2013) 10–15.
[18] A.B. Mattos, T.A. Freitas, L.T. Kubota, R.F. Dutra, Biochem. Eng. J. 71 (2013) 97–104.
[19] B.E. Rapp, F.J. Gruhl, K. Länge, Anal. Bioanal. Chem. 398 (2010) 2403–2412.
[20] J. Lin, Z. Wei, H. Zhang, M. Shao, Biosens. Bioelectron. 41 (2013) 342–347.
[21] K.-J. Huang, D.-J. Niu, J.-Y. Sun, J.-J. Zhu, J. Electroanal. Chem. 656 (2011) 72–77.
[22] A.J. Bard, L.R. Faulkner, Electrochemical Methods: Fundamentals and Applications, John Wiley & Sons, New York, 2000.
[23] P. Yáñez-Sedeño, J.M. Pingarrón, Trends Analyst Chem. 29 (2010) 938–953.
[24] P.J. Lamas-Ardisana, P. Queipo, P. Fanjul-Bolado, A. Costa-Garcia, Anal. Chim. Acta 615 (2008) 30–38.
[25] M. Pumera, A. Merkoci, S. Algeret, Sens. Actuators, B 113 (2006) 617–622.
[26] C. Lynam, N. Gilmartin, A.I. Minett, R. O'Kennedy, G. Wallace, Carbon 47 (2009) 2337–2343.
[27] S. Puertas, M.G. Villa, E. Mendoza, C. Jiménez-Jorquera, J.M. Fuente, C. Fernández-Sánchez, V. Grazu, Biosens. Bioelectron. 43 (2013) 274–280.
[28] M.A. Alonso-Lomillo, O. Domínguez-Renedo, L.D.T.D. Román, M.J. Arcos-Martínez, Anal. Chim. Acta 688 (2011) 49–53.
[29] F. Valentini, A. Amine, S. Orlanducci, M.L. Terranova, G. Palleschi, Anal. Chem. 75 (2003) 5413–5421.
[30] T.T. Nguyen, M. Raupach, L.J. Janik, Clays Clay Miner. 35 (1987) 60–67.
[31] P. Griffiths, J.A.D. Haseth, Fourier Transform Infrared Spectrometry, John Wiley & Sons, New York, 2007.
[32] Z. Pei, H. Anderson, A. Myrskog, G. Dunér, B. Ingemarsson, T. Aastrup, Anal. Biochem. 398 (2010) 161–168.
[33] V. Dugas, A. Elaissari, Y. Chevalier, Surface Sensitization techniques and recognition receptors immobilization on biosensors and microarrays, in: M. Zourob (Ed.), Recognition Receptors in Biosensors, Springer, New York, 2010, pp. 47–134.
[34] G.L. Long, J.D. Winefordner, Anal. Chem. 55 (1983) 713A–724A.
[35] F. Ricci, G. Adornetto, G. Palleschi, Electrochim. Acta 84 (2012) 74–83.
[36] M.P. Hudson, C.M. O'Connor, W.A. Gattis, G. Tasissa, V. Hasselblad, C. M. Holleman, L.H. Gaulden, F. Sedor, E. Magnus Ohman, Am. Heart J. 147 (2004) 546–552.